

# Photochemical & Photobiological Sciences

An international journal

Accepted Manuscript

View Article Online  
View Journal

This article can be cited before page numbers have been issued, to do this please use: T. Kwon, S. Lee, J. Kim, Y. N. Jang, S. Kim, S. K. Mun, C. W. Kim, J. Na and B. J. Kim, *Photochem. Photobiol. Sci.*, 2020, DOI: 10.1039/C9PP00444K.



This is an Accepted Manuscript, which has been through the Royal Society of Chemistry peer review process and has been accepted for publication.

Accepted Manuscripts are published online shortly after acceptance, before technical editing, formatting and proof reading. Using this free service, authors can make their results available to the community, in citable form, before we publish the edited article. We will replace this Accepted Manuscript with the edited and formatted Advance Article as soon as it is available.

You can find more information about Accepted Manuscripts in the [Information for Authors](#).

Please note that technical editing may introduce minor changes to the text and/or graphics, which may alter content. The journal's standard [Terms & Conditions](#) and the [Ethical guidelines](#) still apply. In no event shall the Royal Society of Chemistry be held responsible for any errors or omissions in this Accepted Manuscript or any consequences arising from the use of any information it contains.

# 310 nm UV-LED Attenuates Imiquimod-Induced Psoriasis-like Skin Lesions in C57BL/6 Mice and Inhibits IL-22-Induced STAT3 Expression in HaCaT Cells

Tae-Rin Kwon<sup>1\*</sup>, Sung-Eun Lee<sup>1, 2</sup>, Jong Hwan Kim<sup>1, 2</sup>, You Na Jang<sup>1, 2</sup>, Su-Young Kim<sup>1, 2</sup>, Seok-Kyun Mun<sup>3</sup>, Chan Woong Kim<sup>4</sup>, Jungtae Na<sup>1</sup>, Beom Joon Kim<sup>1, 2†</sup>

<sup>1</sup>Department of Dermatology, Chung-Ang University College of Medicine, Seoul, Korea

<sup>2</sup>Department of Medicine, Graduate School, Chung-Ang University, Seoul, Korea

<sup>3</sup>Department of Otorhinolaryngology-Head and Neck Surgery, Chung-Ang University College of Medicine, Seoul, Korea

<sup>4</sup>Department of Emergency Medicine, Chung-Ang University College of Medicine, Seoul, Korea

**Running title:** 310 nm UV-LED Attenuates Skin Inflammation *In vitro* and *In vivo*

**Funding sources:** This research was supported by the Basic Science Research Program through the National Research Foundation of Korea (NRF) funded by the Ministry of Education (NRF-2017R1D1A1B03030435).

**Conflicts of interest:** None

**Word count:** 6479

**Corresponding author:** Beom Joon Kim, MD, Dept. of Dermatology, Chung Ang University

Hospital 224-1 Heukseok-dong, Dongjak-ku, Seoul 156-755, South Korea

E-mail: beomjoon@unitel.co.kr, Tel: 82-2-6299-1525, Fax: 82-2-823-1049

View Article Online  
DOI: 10.1039/C9PP00444K

## Abstract

Ultraviolet light-emitting diodes (UV-LEDs) are a novel light source for phototherapy. This study aimed to evaluate the therapeutic effects of UV-LEDs on psoriasis. Importantly, 310 nm UV-LEDs have not been studied in psoriasis *in vitro* and *in vivo*. Effects by 310 nm UV-LED and 311 nm narrowband ultraviolet B (NBUVB) irradiation were compared for suppressing IL-22-induced activation of STAT3 expression using cell viability assay, western blotting, and immunocytochemistry. C57BL/6 mice, were topically treated with imiquimod (IMQ) for 6 consecutive days and observed degenerative changes. Test groups were irradiated by 310 nm UV-LED and 311 nm NBUVB. Phenotypic observations, histopathological examinations, and ELISA were conducted with skin and blood samples. STAT3-dependent IL-22 signalling and effects in keratinocytes are negatively regulated by 310 nm UV-LED, which significantly ameliorated IMQ-induced psoriasis-like dermatitis development and reduced Th17 cytokine levels (IL-17A, IL-22) in serum and dorsal skin. Histopathological findings showed decreases in epidermal thickness and inflammatory T-cell infiltration in the UV-LED-irradiated groups. Quantitative PCR confirmed UV radiation energy-dependent decrease in IL-17A and IL-22 mRNA levels. The results demonstrated that UV-LEDs had anti-inflammatory and immunoregulatory effects. So, UV-LED phototherapy inhibits psoriasis development by suppressing STAT3 protein and inflammatory cytokines and could be useful in treating psoriasis.

**Keywords:** 310 nm, UV-LED, psoriasis, phototherapy

## Introduction

Psoriasis, a T-cell-mediated chronic inflammatory immune disease, is characterized by overgrowth and poor differentiation of epidermal keratinocytes and major white blood cell infiltration<sup>1</sup>. Histological changes include epidermal hyperplasia and aberrant differentiation, granule depletion, dermal inflammatory infiltration, and thickened epidermis due to increased dermal vasculature<sup>2</sup>. Psoriasis affects  $\leq 2\%$  of the population in Nordic countries and 0.1–0.3% in Asian countries, and its exact cause is not well established<sup>3</sup>. Although psoriasis pathogenesis is not fully understood, many cytokines, including IL-6, IL-17A, IL-17F, IL-22, IL-23, and TNF- $\alpha$ , and cells including dendritic cells (DC), neutrophils, endothelial cells, and fibroblasts play an important role in psoriasis maintenance and development<sup>4</sup>.

Phototherapy is the only treatment option for patients with contraindications due to immune system changes, such as HIV, internal malignancy, or pregnancy<sup>5</sup>. UVB is highly cost effective, which is important due to rising healthcare costs<sup>6</sup>. Current psoriasis therapies include topical psoralen treatments with ultraviolet A photochemotherapy, steroids, retinoids, immunosuppressants, vitamin D3 derivatives, and biological therapeutics<sup>7</sup>. However, most therapies have various side effects and require long-term administration. Therefore, a new effective drug without side effects is urgently needed.

The elimination of psoriasis by NB-UVB is associated with type I and type II interferon signal inhibition and Th1 pathway down-regulation in lesional epidermis<sup>8</sup>. NB-UVB inhibits signal transducer and activator of transcription factor 3 (STAT3) phosphorylation, thereby reducing transcriptional target expression (e.g., the antimicrobial peptide human  $\beta$ -defensin). Recently, UV light-induced ubiquitination and down-regulation of IFNAR1, a type I interferon receptor, mediated ultraviolet (IR) responses in imiquimod-induced psoriasis models<sup>9</sup>. Unlike wild-type mice, psoriatic inflammation in IFNAR1-deficient mice showed

no improvement by ultraviolet light. Similarly, IFNAR1 was ubiquitinated and down-regulated by ultraviolet light in human psoriatic skin.

Interleukin (IL)-22 is a cytokine primarily released by T helper (Th) 17 and Th22 lymphocytes, which are involved in psoriasis pathogenesis<sup>10</sup>. In psoriasis, IL-22 is involved in altered growth and differentiation processes observed in the epidermis and induces inflammatory molecules in keratinocytes<sup>11</sup>. STAT3 is a key mediator of IL-22 signalling, and its full activation requires the phosphorylation of tyrosine (Tyr) 705 and serine (Ser) 727 residues<sup>12</sup>. Both phosphorylation sites were phosphorylated in lesional psoriatic skin<sup>13</sup>. This study aimed to identify downstream effects on target molecules and human keratinocytes that could inhibit IL-22-induced STAT3 phosphorylation of (Ser) 727 due to abnormal STAT3 activation in psoriatic epidermis.

We examined whether 310 nm UV-LEDs could inhibit imiquimod (IMQ)-induced psoriasis-like skin inflammation in mice. Our results demonstrate that 310 nm UV-LEDs can treat psoriasis-like skin inflammation through inhibiting pro-inflammatory responses and down-regulating STAT3 expression. These results imply that 310 nm UV-LEDs can be used to treat immune-related inflammatory skin diseases.

## Materials and Methods

### *Cell culture and LED treatment*

The human keratinocyte cell line HaCaT was grown in Dulbecco's Modified Eagle's Medium (DMEM) supplemented with 10% fetal bovine serum, 2 mM L-glutamine, 100 U/mL penicillin, and 100 µg/mL streptomycin at 37 °C in a humidified incubator with 5% CO<sub>2</sub>. Cells were pre-treated with 100 ng/mL IL-22 for 1 h, radiated by UV-LEDs at indicated

energy levels, and used after 24 h. 310 nm LED devices were provided by the Seoul Viosys Institute (Ansan, Korea). HaCaT cells were irradiated using a novel UV-LED device for *in vitro* testing (130 × 90 mm). Power fluences of 310 nm (171  $\mu\text{W}/\text{cm}^2$ ) were delivered to a platform located 50 mm below the LED arrays<sup>14</sup>. Before UV-LED (310 nm) irradiation, cultures were rinsed in phosphate-buffered saline (PBS) and irradiated with the indicated fluencies in PBS to avoid absorption by phenol red in the culture medium. All groups were kept in PBS at room temperature to ensure equal treatment conditions.

### ***CCK-8 assay***

Human HaCaT keratinocytes were plated at a density of  $1.0 \times 10^4$  cells/well in 96-well plates, and their proliferation was measured by cholecystokinin (CCK)-8 assay (Dojindo, Rockville, MD, USA). Cells ( $2 \times 10^4$  cells/well) were pre-treated with IL-22 (100 ng/mL) for 1 h, then irradiated with 310 nm UV-LEDs and 311 nm narrowband ultraviolet B (NBUBV) for radiant exposures of 30, 40, and 50  $\text{mJ}/\text{cm}^2$  for 24 h. CCK-8 solution (10  $\mu\text{L}$ ) was added to cells in 1 mL DMEM and incubated for 2 h at 37 °C. Absorbance was measured at 450 nm using a microplate reader (SpectraMax 340; Molecular Devices, Sunnyvale, CA, USA).

### ***Immunocytochemistry***

HaCaT cells were seeded onto chamber slides at  $2.0 \times 10^4$  cells/500  $\mu\text{L}$  chamber and irradiated with 310 nm UV-LEDs. After 24 h, cells were treated with 4% paraformaldehyde for 10 min and 0.1% Triton X-100 for 5 min. Cultured HaCaT cells were incubated with anti-(pS-STAT3) (1:1000, ab86430, Abcam, Cambridge, MA, USA) at 4 °C overnight and with fluorescein isothiocyanate (FITC)-labelled goat anti-rabbit IgG (1:1000, NB730-F, Novus Biologicals, Centennial, CO, USA). Nuclei were counterstained with 40,6-diamidino-2-

phenylindole (DAPI). Immunostained cells were mounted with medium containing DAPI and visualized using an Olympus FLUOVIEW FV10i confocal microscope (Olympus, Waltham, MA, USA).

### ***Western blotting***

Total protein was extracted from cell lysates of mouse back skin, and western blotting was performed. Protein extracts were prepared using RIPA buffer (50 mM Tris-HCl pH 7.2, 150 mM NaCl, 1% NP40, 0.1% sodium dodecyl sulfate (SDS), 0.5% DOC, 1 mM phenylmethylsulfonyl fluoride, 25 mM MgCl<sub>2</sub>, and phosphatase inhibitor cocktail). Protein amounts in extracts were quantitated using a Bio-Rad DC Protein Assay Kit II (Bio-Rad, Hercules, CA, USA). Equal protein amounts were resolved on 10% SDS-PAGE gels and electrotransferred to nitrocellulose membranes. After blocking with 5% non-fat milk, membranes were probed with specific antibodies against ERK (1:1000, 9102, Cell Signaling Technology, Danvers, MA, USA), phosphorylated (p)ERK (1:1000, 9101, Cell Signaling Technology), serine 727 (pS-STAT3) (1:1000, ab86430, Abcam), total STAT3 (1:1000, 9139, Cell Signaling Technology), S100A9 (1:1000, NB110-89726, Novus Biologicals), and  $\beta$ -actin (1:1000, 4967, Cell Signaling Technology). After washing, membranes were incubated with HRP-conjugated anti-mouse or anti-rabbit secondary antibodies. Immunoreactive signals were detected using enhanced chemiluminescence reagents (Amersham Pharmacia, Piscataway, NJ, USA). Protein levels were compared to loading controls.

### ***Ethic statement***

The mice were treated according to the regulations of the Institutional Animal Care and Use

Committee of Chung Ang University, Korea, which conform to the National Institutes of Health guidelines. All animal procedures were performed in accordance with the Guidelines for Care and Use of Laboratory Animals of Chung-Ang University and approved by the Animal Ethics Committee of Chung-Ang University IACUC (Approval No. 201800019).

### ***Mice and IMQ treatment***

Nine-week-old C57BL/6 mice were purchased from Central Laboratory Animal, Inc. (Seoul, Korea) and kept under specific pathogen-free conditions. Mice were provided with standard laboratory mouse chow and water. After mice were anesthetized with Zoletil 50 (50 mg/kg; Virbac Laboratories, Carros, France) and xylazine (10 mg/kg), fur on their dorsal surface was shaved using an electric mouse clipper. Mice received a daily topical dose of 62.5 mg of commercially available IMQ cream (5%; Aldara, 3M Pharmaceuticals, Loughborough, UK) on the shaved back skin for 6 days, then were exposed to UV-LED (310 nm) and NB-UVB irradiation three times per week (Fig. 2A). with the UV-LED device contained an *in vivo* test module (160×200 mm). For *in vivo* experiments, the intensity of the 310 nm UV-LED was 80  $\mu\text{W}/\text{cm}^2$  at a distance of 20 cm and was applied three times per week for 10 min 40 s with 50  $\text{mJ}/\text{cm}^2$  total energy delivered per exposure. *In vitro* experiments used 311–313 NB-UVB at 2–3 cm distance for 3 min with 630  $\text{mJ}/\text{cm}^2$  total energy. Mice were randomly assigned to five groups (n=6 per group): G1, Normal; G2, Control (IMQ only); G3, 20  $\text{mJ}/\text{cm}^2$  of 310 nm; G4, 50  $\text{mJ}/\text{cm}^2$  of 310 nm; and G5, 311 nm NB-UVB lamp.

### ***Skin inflammation severity scoring***

To score inflammation severity on ear skin, an objective scoring system was developed based on the clinical Psoriasis Area and Severity Index (PASI). Erythema, scaling, and thickening



were scored independently from 0–4 as follows: 0, none; 1, slight; 2, moderate; 3, marked; 4, very marked. The erythema level was scored using a scoring table with red blemishes. The cumulative score (erythema plus scaling plus thickening) served to indicate inflammation severity (scale: 0–12), as described previously<sup>15</sup>.

### ***Measurement of inflammatory cytokine levels***

Mice were anesthetized and their eyes were bled at 6 days. Sera were stored at –80 °C. IL-1 $\beta$ , IL-6, IL-17A, IL-22, TNF- $\alpha$ , and IFN- $\gamma$  levels were measured in mouse sera by Enzyme-Linked Immunosorbent Assay (ELISA) (eBioscience, San Diego, CA, USA) in serial two-fold dilutions for treated or control mice according to manufacturer instructions.

### ***RNA isolation and quantitative real-time polymerase chain reaction (PCR) analysis***

Total RNA was extracted from dorsal skin tissues and isolated using Trizol® reagent (Invitrogen, Carlsbad, CA, USA) according to the manufacturer's instructions. Synthesis of cDNA was performed according Takara PrimeScript™ RT Reagent Kit instructions (Takara, Tokyo, Japan). TB Green® Premix Ex Taq™ II (Takara, Tokyo, Japan) was used for real-time PCR, and all reactions were repeated three times under the following conditions: initial denaturation at 95 °C for 30 s, followed by 40 cycles at 95 °C for 5 s and 60 °C for 30 s. Reactions were conducted in triplicate on a CFX96™ Real-Time System (Bio-Rad, Hercules, CA, USA) with no template control reactions for each primer set. Real-time PCR primers are listed in Table 1.

### ***Histopathological analysis***

Mice were sacrificed 6 days after the start of the experiment. Skin specimens were fixed in 4%

paraformaldehyde, embedded in paraffin, and cut into 5  $\mu\text{m}$ -thick sections, which were stained with haematoxylin and eosin (H&E) and toluidine blue according to established procedures for the histological analysis of back and ear skin. Skin specimens were stained using antibodies for immunohistological analysis according to a previously published method. Sections were stained with monoclonal antibodies against serine 727 (pS-STAT3) (1:100, ab86430, Abcam) and S100A9 (1:100, NB110-89726, Novus Biologicals) as described previously.

### ***Immunofluorescence analysis***

Sections were blocked at room temperature for 2 h in PBS containing 0.2% Triton X-100 and normal horse serum, then stained with rabbit monoclonal antibodies against pS-STAT3 and S100A9 (1:200) during incubation overnight at 4 °C. Then, sections were washed thrice for 5 min each with 0.2% Triton X-100 in PBS, incubated at room temperature with FITC-conjugated anti-goat anti-rabbit (1:200, sc-2012, Santa Cruz Biotechnology, Santa Cruz, CA, USA) and Texas red (TR)-conjugated anti-goat anti-rabbit (1:200, sc-2780, Santa Cruz Biotechnology) for 30 min, and counterstained for 5 min with DAPI.

### ***Statistical analysis***

Data are presented as the mean  $\pm$  standard deviation (SD) of at least three separate experiments. Statistical significance was calculated by one-way ANOVA followed by Duncan's multiple range test. P-values of  $p < 0.05^*$ ,  $p < 0.01^{**}$ , and  $p < 0.001^{***}$  were considered statistically significant. Results are expressed as mean  $\pm$  SD ( $n=6$ ). For direct comparisons between specific *in vivo* study groups, statistical significance was determined with one-way ANOVA followed by post-hoc Tukey test using SPSS software (SPSS Inc.,

Chicago, IL, USA).

View Article Online  
DOI: 10.1039/C9PP00444K

## Results

### *310 nm UV-LED Suppresses IL-22-Induced STAT3 phosphorylation in Human Keratinocytes*

To confirm the inhibitory effect of 310 nm UV-LED on psoriasis-like skin inflammation, we determined the anti-inflammatory effect of 310 nm UV-LED on keratinocyte cell lines, which are the main cell type stimulated by IMQ in this mouse model. In vitro 310 nm UV-LED irradiation devices were prepared (Fig. 1A). The 310 nm UV-LED and 311 nm NBUVB power densities were 171 and 3.5 mW/cm<sup>2</sup>, respectively. To determine an irradiation range for investigating the effects of UV-LEDs on HaCaT cell viability, we used 310 nm UV-LED and 311 nm NBUVB irradiation at radiant exposures of 30, 40, and 50 mJ/cm<sup>2</sup>. CCK-8 assay results showed that irradiation with 310 nm UVB-LED and 311 nm NBUVB up to 50 mJ/cm<sup>2</sup> had no cytotoxic effects on HaCaT cells. The viability of both irradiation types was suppressed up to 80% by adding 100 ng/mL IL-22 to cultures, indicating that 310 nm UV-LED irradiation suppressed IL-22-induced cell growth (Fig. 1B). HaCaT cells were activated by IL-22, which is involved in psoriasis pathogenesis, and western blot measured pSTAT3 expression, which participates in Th17 cell differentiation and psoriasis. As shown in Fig. 1C, IL-22 induced a time-dependent increase on pERK and pSTAT3 expression. Furthermore, we determined whether 310 nm UV-LED had an effect on STAT3 suppression, which is crucial for Th17 cell differentiation and psoriasis pathogenesis. Figure 1D shows that 310 nm UV-LED inhibited STAT3 activation (pSTAT3) in IL-22-stimulated HaCaT cells. We also confirmed the effect of UV-LED irradiation on STAT3 nuclear translocation using

immunocytochemistry. After IL-22 stimulation, cytosolic STAT3 was translocated to the nucleus; this was inhibited by 310 nm irradiation (50 mJ/cm<sup>2</sup>) (Fig. 1F).

These results suggest that 310 nm irradiation inhibits the STAT3 signalling pathway in keratinocytes, which could result in psoriasis inhibition in mice. Consistent with the importance of STAT3 levels in regulating IL-22 response, HaCaT cell pre-treatment with UV-attenuated STAT3 phosphorylation in response to IL-22 suggested that 310 nm UV-LED can suppress STAT3 signalling.

### ***310 nm UV-LED irradiation reduces IMQ-induced psoriasiform lesions in mice***

To investigate whether 310 nm UV-LED has a beneficial effect on psoriasis, we irradiated the psoriasis mouse model with 310 nm UV-LED and 311 nm NBUVB. Psoriasis was induced in mice by topical IMQ application. Consecutive IMQ application for 6 days on C57BL/6 mouse back skin induced skin inflammation showing redness, thickness, and scale, which was similar to human psoriasis. After inducing psoriasiform skin inflammation, subsequent irradiation with 310 nm UV-LED or 311 nm NBUVB was conducted for 3 days. Both treatments ameliorated psoriasiform skin inflammation at the macroscopic level (Fig. 2B). A modified scoring system based on PASI used in human psoriasis was applied to evaluate skin inflammation severity. Erythema appeared one day after IMQ application, and it reached a peak after 6 days. Both thickness and scaling were observed after 3 days and increased gradually until day 6. The normal group showed no signs of inflammation on the dorsal skin or right ear pinna, whereas the IMQ-treated area showed erythema and thickened skin layers. Interestingly, 50 mJ/cm<sup>2</sup> of both 310 nm UV-LED and NB-UVB irradiation alleviated skin conditions. Severity examination showed that 310 nm UV-LED reduced skin thickness and erythema within a day after administration. The cumulative PASI score was 20

mJ/cm<sup>2</sup> of 310 nm UV-LED-irradiated mice ( $6.00 \pm 0.68$ ), followed by 50 mJ/cm<sup>2</sup> of 310 nm UV-LED ( $5.33 \pm 0.42$ ,  $p < 0.01$ ), 311 nm NBUVB ( $6.00 \pm 0.42$ ), and IQM-only mice ( $7.17 \pm 0.31$ ) (Fig 2C-E). Significant differences were not observed in animal body weights during the study period. The spleen weight to body weight ratio for mice of different treatment groups was recorded on the 6 day. The IMQ group showed a drastic increase in spleen weight to body weight ratio compared to the normal group, indicating psoriasis induction after IMQ application, while different treatment groups resulted in reduced spleen weight to body weight ratio. No statistically significant difference was observed between treatment groups (Fig 3A). These results suggested that 310 nm UV-LED irradiation markedly reduced epidermal layer thickness and attenuated IMQ-induced psoriasis.

### ***310 nm UV-LED attenuates the IMQ-induced inflammatory response***

We then investigated the impact of 310 nm UV-LED on inflammatory infiltration. IMQ up-regulated psoriasis-associated cytokine levels in mouse serum, indicating systemic immunity activation. It was found that 310 nm UV-LED pre-treatment down-regulated cytokine serum levels of Th1 and IL-23/Th17 axis, including IL-1b, IL-6, IL-17A, IL-22, TNF- $\alpha$ , and IFN- $\gamma$ . Circulating IL-1 $\beta$  levels increased over 8.5-fold; IL-6, 1.9-fold; IL-17A, 2.0-fold; IL-22, 1.66-fold; TNF- $\alpha$ , 3.01-fold; and IFN- $\gamma$ , 3.68-fold. In 310 nm UV-LED-treated mice, IL-1b, IL-6, IL-17A, IL-22, TNF- $\alpha$ , and IFN- $\gamma$  serum levels were significantly decreased ( $p < 0.05$ ). (Fig. 3B-G). Compared to the IMQ group, 310 nm UV-LED or 311 nm NBUVB irradiation reduced IFN- $\gamma$  levels by 2.74-fold and 2.32-fold, respectively, indicating that 50 mJ/cm<sup>2</sup> of 310 nm UV-LED more highly suppressed IFN- $\gamma$  levels than 311 nm NBUVB.

Histopathology of different treatment groups in the IMQ-induced psoriatic plaque model

was performed to observe psoriatic features and treatment effects in skin recovery. H&E staining images of back and ear skin tissues from different treatment groups are presented. In the IMQ-induced group, histological examination of the H&E-stained sections showed epidermal thickening and elongation of rete ridges, reflecting a hyper-proliferative state with hyperkeratosis and parakeratosis (Fig. 4A). The 310 nm UV-LED group showed an increase in IL-1 $\beta$  compared to the 311 nm NBUVB group.

The effect of 310 nm UV-LED and 311 nm NBUVB on inflammatory cytokine mRNA expression in the back skin tissue of the IMQ-induced psoriasis mouse model is shown in Figure 4B-G. The expression levels of *IL-1b*, *IL-6*, *IL-17A*, *IL-22*, *TNF- $\alpha$* , and *IFN- $\gamma$*  were markedly increased in the skin tissues of the negative control group relative to the control group. However, 310 nm UV-LED and NBUVB irradiation on the exposed skin of IMQ psoriatic mice significantly reduced the expression of *IL-1 $\beta$* , *IL-6*, *IL-17A*, *IL-22*, *TNF- $\alpha$* , and *IFN- $\gamma$* , when compared to the negative control group. These results indicated that inflammatory cytokine production was significantly inhibited by 310 nm UV-LED and NBUVB irradiation.

### ***STAT3 signalling mediated the inhibitory effects of 310 nm UV-LED in a psoriasis mouse model***

We next sought to determine whether STAT3 down-regulation contributes to therapeutic effects by 310 nm UV-LED using an IMQ-induced psoriasiform inflammation mouse model. Histopathological examination detected increased epidermal hyperproliferation and altered keratinocyte differentiation in IQM-induced psoriasiform skin inflammation. IMQ application led to epidermal hyperplasia with strong epidermal thickening, hyperkeratosis with elongated rete ridges, parakeratosis, and cellular dermis infiltration. Therefore,

immunohistochemical staining was performed to confirm changes in quantities of S100A9 protein, which is a psoriasis marker. S100A9 expression is transiently induced in keratinocytes after epidermal injury and induced by pro-inflammatory cytokines in psoriasis. S100A9 expression was reduced in the ear and back skin lesions of 310 nm UV-LED-treated mice, suggesting that 310 nm UV-LED reduces IMQ-induced keratinocyte proliferation (Fig. 5A). S100A9 expression in keratinized epidermal cells was observed throughout the epidermal layer of lesions and decreased in 310 nm UV-LED-treated mice. Consequently, immunohistochemical analysis showed that S100A9 levels were significantly reduced in the 310 nm UV-LED and 311 nm NBUVB group compared to the negative control group. Furthermore, S100A7, S100A9, and KRT16 mRNA expression was significantly decreased during 310 nm UV-LED and 311 nm NBUVB therapy (Fig. 5B-D). Thus, as observed in the psoriatic IMQ-mouse model, 310 nm UV-LED suppresses psoriasiform dermatitis in mice, which is accompanied by down-regulation of the Th17 pathway.

STAT3 has emerged as an important regulator of keratinocytes and Th17 cell differentiation<sup>16</sup>. Western blotting was used to investigate whether 310 nm UV-LED influences Th17 cells by inhibiting STAT3 signalling in psoriasis, and increased STAT3 phosphorylation was found in IMQ-induced skin lesions. The levels of phosphorylated STAT3 forms decreased in 310 nm UV-LED and 311 nm NBUVB-irradiated mice (Fig. 6A and B). Next, we performed immunofluorescent staining for S100A9 and phosphorylated STAT3 on mouse back skin and observed a remarkable decrease in S100A9 and STAT3 protein expression in the 310 nm UV-LED group compared with that in the 311 nm NBUVB group (Fig. 6C and D). Taken together, these results suggest that 310 nm UV-LED irradiation effectively ameliorates IMQ-induced lesional *psoriatic* skin via the STAT3 signalling pathway.

## Discussion

Phototherapy is a highly effective treatment modality for the chronic inflammatory skin disease psoriasis<sup>17</sup>. Lymphocytes and epidermal keratinocytes, leading to immunity, interfere with pathological changes that characterize psoriasis<sup>18</sup>. UVB radiation modulates cytokine expression in effector cells in human skin, resulting in local and systemic immunosuppression<sup>19</sup>. This immunomodulatory effect is simultaneously favourable and disadvantageous because it suppresses reactivity to self-antigens generated due to ultraviolet exposure; however, it can promote skin cancer induction<sup>20</sup>. Recent studies have shown that the efficacy of UVB treatment in psoriasis can be explained by immunosuppressive effects<sup>21</sup>,<sup>22</sup>. This study showed that UVB treatment not only reduced the number of T cells infiltrating psoriatic skin, but also decreased the predominance of pro-inflammatory cytokine in lesions. Our previous paper demonstrates that the anti-inflammatory effect of 310 nm UV-LED is at least partially mediated by inhibiting epidermal keratinocyte proliferation<sup>14</sup>. In this study, the antiproliferative mechanisms of 310 nm UV-LED compared with NB-UVB lamps were further studied. In particular, we provided experimental data validating the therapeutic potential of 310 nm UV-LEDs by using them in immunomodulation and in vitro and in vivo models.

IL-22 secreted by Th17 cells induces STAT3 phosphorylation. Phosphorylated STAT3 translocates to the nucleus and induces transcription of genes involved in the described function. NB-UVB inhibits the STAT3 phosphorylation and reduces STAT3 target gene expression<sup>23</sup>. Additionally, selective inhibition of STAT3 phosphorylation is another method for targeting the Th17 pathway. Constitutive STAT3 activation is associated with cancer



initiation<sup>24</sup>, proliferation<sup>25</sup>, angiogenesis promotion<sup>26</sup>, and chronic inflammatory skin disease<sup>27</sup>. In this study, we examined whether IL-22 induces dose-dependent and time-dependent STAT3 phosphorylation in HaCaT keratinocytes. Particularly, our experiments showed that 310 nm UV-LED irradiation induced cytotoxicity in IL-22-induced HaCaT cells. Therefore, 310 nm UV-LED may be widely used to treat many other inflammatory skin diseases. In vitro experiments show that stimulated cells are more sensitive to 310 nm UV-LED than to 311 nm lamps, suggesting that the former can inhibit Th17 cell activity by a molecular mechanism involving inhibition or interruption of the IL-22-induced STAT3 signalling pathway. It has been shown that 310 nm UVB irradiation induces an immunosuppressive response in the skin through the STAT3 signalling pathway. Thus, an immunosuppressive response induced by 310 nm UVB irradiation may be effective in ameliorating psoriasis symptoms.

UV-LED has various features which are advantageous for analysis, such as being compact, of single wavelength, the ability to select wavelengths, ease of switching properties on and off, directionality of light, long service life, low power consumption, mercury free, etc. In particular, in this study, it was confirmed that the inflammatory skin diseases such as psoriasis can be controlled with less energy by comparing the safety and efficacy compared to the conventional NB-UVB method. However, further experimentation should be conducted as to whether narrow wavelengths such as 310 nm can be more effective.

The main advantages of UV-LEDs include wavelength tunability, single peak emission, low power consumption, a long lifetime, and small form factor. Kemeny et al. observed in clinical trials that UVB-LED devices are effective treatments for plaque psoriasis<sup>28</sup>. However, subsequent studies did not confirm these preclinical results. Therefore, we investigated

psoriasis suppression and UV-LED irradiation as a treatment for psoriasis using an animal model. We established IMQ-induced psoriasis-like skin lesions in C57BL/6 mice and found that 310 nm UV-LED significantly improved keratinocyte proliferation, inflammatory infiltration, and total, histological, cellular, and molecular changes. Improved recovery of inflammatory cytokines was reduced by 310 nm UV-LEDs, which generally displayed slightly higher benefits at 50 mJ/cm<sup>2</sup> than at 25 mJ/cm<sup>2</sup>. Based on this data, 50 mJ/cm<sup>2</sup> 310 nm UV-LED is more suitable for psoriasis. However, the optimal dose should be examined in further studies. In vivo, Th17 cell differentiation and IL-17 secretion in psoriatic lesions were suppressed by 310 nm UV-LEDs, which thus weakened psoriatic inflammation by interfering with Th17 cell function. However, blood cytokine levels did not correlate with cytokine mRNA levels such as TNF- $\alpha$  or IL-1. There are many complicated and varied post-transcriptional mechanisms involved in turning mRNA into protein that are not yet sufficiently well defined to be able to compute protein concentrations from mRNA; second, proteins may differ substantially in their in vivo half lives; and/or third, there is a significant amount of error and noise in both protein and mRNA experiments that limit our ability to get a clear picture. The second reason identified above for not being able to detect TNF- $\alpha$  or IL-1 in the circulation is the presence of inhibitors that not only bind and inactivate the cytokines but also interfere with their detection. In addition, multiplexed cytokine immunoassays are easily applied to biomarker discovery and routine toxicity studies to measure blood cytokines. However, cytokines pose several challenges as safety biomarkers because of a short serum half-life; low to undetectable baseline<sup>29</sup>. Further studies are needed to resolve these uncertainties.

In summary, although it has not yet been demonstrated that inhibition of STAT3

phosphorylation is sufficient to improve psoriasis clinically, several strategies have been developed for the inhibition of STAT3 phosphorylation and activation.

STAT3 signalling is up-regulated in both psoriasis and IMQ-induced psoriasis-like lesions. Our study suggests that 310 nm UV-LED irradiation directly affects many processes associated with STAT3 signalling in inflammation similar to IMQ-induced psoriasis and effectively improves IMQ-induced lesional psoriatic skin through the STAT3 signalling pathway. The 310 nm UV-LED used to target IL-17A for psoriasis treatment maintains an adequate balance of T cell differentiation. Based on the results observed in this study, we suggest that reducing inflammatory cell differentiation and cytokine secretion through the STAT3 signalling pathway may be an alternative treatment strategy for psoriasis. However, further research is needed to understand the cellular effects of 310 nm UV-LED, identify the exact molecular pathway that it influences, and determine whether the decreased cytokine expression is caused by the direct effect of its irradiation on the production capacity of other cell types or by the reduction of cytokine-producing inflammatory cells. Further investigation will be required to determine the exact mechanism whereby psoriasis associated gene expression is controlled by STAT3.

These in vitro and in vivo studies suggest that 310 nm UV-LEDs enhance the phenotypic and histopathological characteristics of psoriatic skin and reduce the levels of TNF- $\alpha$ , IL-17 and IL-22, therefore indicating that the developed device holds improved anti-psoriatic potential. Thus, our study showed that 310 nm UV-LEDs are effective in treating psoriasis and are clinically beneficial.

In conclusion, we demonstrated that 310 nm UV-LED alleviates IMQ-induced psoriasis-like inflammation by reducing inflammatory cell differentiation and cytokine secretion,

specifically by directly inhibiting Th17 cell differentiation and IL-17A secretion. These findings present new avenues treating inflammatory skin diseases and suggest that 310 nm UV-LEDs could serve as a candidate modality for inhibiting local inflammation in psoriasis.

### Acknowledgements

This research was supported by the Basic Science Research Program through the National Research Foundation of Korea (NRF) funded by the Ministry of Education (NRF-2017R1D1A1B03030435).

### Competing financial interests

Authors have no potential conflicts of interest to disclose.

### Figure legends

**Fig. 1 Effects of 310-nm UV-LED on IL-22-induced STAT3 activation in HaCaT cells** (a) Emission spectra of 310 nm UV-LED. (b) UV-LEDs cytotoxicity to HaCaT cells was measured by CCK-8 assays. Cells in 96-well microplates ( $2 \times 10^4$  cells/well) were irradiated with 310 nm UV-LED and 311 nm NB-UVB (30, 40, 50, and 60 mJ/cm<sup>2</sup>) for 24 h (black bars). Cells ( $2 \times 10^4$  cells/well) were also pre-treated with IL-22 (100 ng/mL) for 1 h before radiation (grey bars). Unirradiated cells were the control group. Values are mean $\pm$ SD of three independent experiments. (c) Cell lysates were prepared, and serine 727 phosphorylation (pS-STAT3) was determined in cells stimulated by IL-22 (100 ng/mL) for 0, 5, 10, 30, 60, 120, and 180 minutes. (d) Cells were pre-treated with IL-22 (100 ng/mL for 1 h and irradiated with UV-LEDs at indicated energy levels for 24 h. Cell lysates were prepared and subjected

to western blotting for pS-STAT3, p-ERK, and  $\beta$ -actin. (e) Relative protein ratios were determined as band intensities with pS-STAT3 and p-ERK ratios in each irradiation group relative to the control. Significant differences from the control group are indicated by \* $P < 0.05$ , \*\* $P < 0.01$ , and \*\*\* $P < 0.001$  versus unirradiated cells. (f) Representative images of immunocytochemical staining by anti-pS-STAT3 (green) for pS-STAT3 in HaCaT cells irradiated with indicated energy levels of 310 nm (50 mJ/cm<sup>2</sup>) for 24 h. Cells were counterstained with DAPI (blue) before mounting. Significant differences from the control group are indicated as \* $P < 0.05$ , \*\* $P < 0.01$ , and \*\*\* $P < 0.001$  versus unirradiated cells.

### Fig. 2 Experimental induction of imiquimod-induced psoriasis-like skin inflammation

**and clinical changes in imiquimod (IMQ)-treated mouse skin** The back skin and right ear of mice were treated with commercially available IQM cream (5%; Aldara, 3M Pharmaceuticals, UK) for 6 consecutive days at a daily dose of 80 mg, which contained 4 mg of the active compound. After application, mice were exposed to UV-LED (310 nm) and NB-UVB every other day. (b) Mice were divided into five groups: G1, Normal; G2, Control (IMQ-applied only); G3, 310 nm 20 mJ/cm<sup>2</sup>; G4, 310 nm 50 mJ/cm<sup>2</sup>; and G5, NB-UVB. Normal mice (left) showed no changes in skin lesions. IMQ-treated mice showed psoriasis-like skin lesions with erythema, thickness, and scale. The picture is representative of the six IMQ group mice. (c, d, e) Psoriasis-like skin lesions were clinically evaluated by PASI scores: erythema increased from day 1 to 6, scaling was observed on day 3 and gradually increased until day 6, and the thickness was observed to increase from day 2 to 6. Data are presented as means $\pm$ SD of changes in values. \*\* $p < 0.01$  compared to the controls (n=6).

### Fig. 3 Effects of UV-LED irradiation on serum cytokine levels in imiquimod (IMQ)-

**treated mice** (a) Mice were sacrificed on day 6 for serum collection after 6 days. Spleen sizes were weighed at sacrifice and compared by direct viewing of representative images. Bar graphs represent the mean $\pm$ SD, with six mice per group. Data shown are representative of three experiments. The serum levels of (b) IL-1 $\beta$ , (c) IL-6, (d) IL-17A, (e) IL-22, (f) TNF- $\alpha$ , and (g) IFN- $\gamma$  were measured. Inflammatory cytokine levels were measured using ELISA kits. Data are presented as means $\pm$ SD of changes in values. \* $p$ <0.05 and \*\* $p$ <0.01 compared to the controls (n=6).

**Fig. 4 Improvement of the imiquimod-induced psoriasiform dermatitis in mice by 310-nm UV-LED is associated with suppression of Th cell-associated inflammatory cytokines** (a) H&E staining of the IMQ-treated back skin section shows psoriasis-like changes including scaling, epidermal thickness, keratinocyte hyperproliferation, and granulocyte infiltration compared to control back and ear skin. A representative picture of six mice is shown. H&E-stained paraffin sections were observed at original magnification ( $\times$ 100). Normal control animals received neither IMQ nor vehicle cream. The mRNA levels of (b) *IL-1 $\beta$* , (c) *IL-6*, (d) *IL-17A*, (e) *IL-22*, (f) *TNF- $\alpha$* , and (g) *IFN- $\gamma$*  were revealed by real-time quantitative RT-PCR (qRT-PCR). Data are presented as means $\pm$ SD of changes in values. \* $p$ <0.05 and \*\* $p$ <0.01 compared to the controls (n=6).

**Fig. 5 Improvement of psoriasis-like skin disease via S100A9 suppression in imiquimod-induced mice after treatment with 310 nm UV-LED.** (a) Immunohistochemical analysis was performed for S100A9 protein in the back and ear skin of psoriatic mice, and UV-LED irradiation could effectively decrease S100A9 protein expression ( $\times$ 100). The mRNA levels of (b) *S100A7*, (c) *S100A9*, and (d) *Keratin 16* were

revealed by real-time quantitative RT-PCR (qRT-PCR). The data are presented as means $\pm$ SD of changes in values. \* $p < 0.05$  and \*\* $p < 0.01$  compared to the controls (n=6).

**Fig. 6 Irradiation of 310 nm UV-LED suppressed skin inflammation via STAT3/S100A9 in imiquimod-induced mice.** (a) Tissue extracts from mouse back skins were prepared and blotted to evaluate pS-STAT3, total STAT3, and S100A9 expression. (b) Relative protein ratios were determined as band intensities with ratios of pS-STAT3 and S100A9 in each irradiation group relative to the control. Significant differences from the control group are \* $P < 0.05$ , \*\*\* $P < 0.001$  versus the control group. (c) S100A9 and (d) pS-STAT3 protein localization was visualized in each group under a fluorescence microscope after staining with each antibody and FITC-labelled secondary antibody (green). The cell nuclei were stained with DAPI ( $\times 100$ ). Images are representative of three independent experiments.

## References

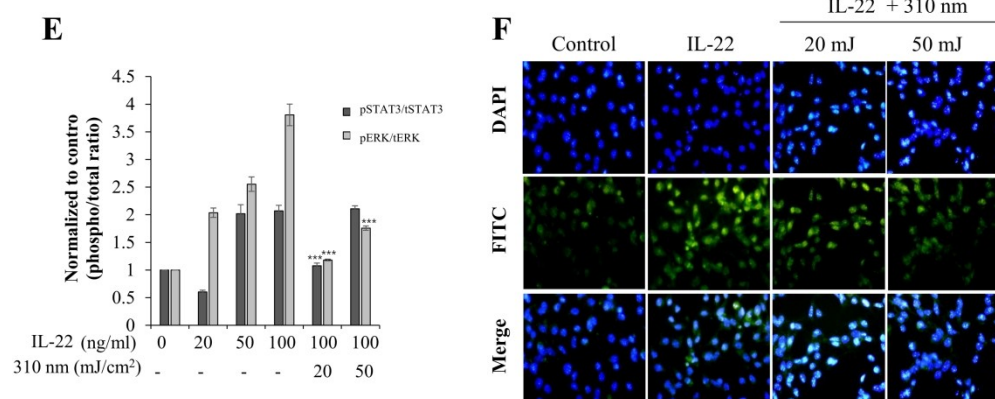
1. M. A. Lowes, A. M. Bowcock and J. G. Krueger, Pathogenesis and therapy of psoriasis, *Nature*, 2007, **445**, 866-873.
2. C. E. Griffiths and J. N. Barker, Pathogenesis and clinical features of psoriasis, *Lancet*, 2007, **370**, 263-271.
3. H. Zachariae, R. Zachariae, K. Blomqvist, S. Davidsson, L. Molin, C. Mork and B. Sigurgeirsson, Treatment of psoriasis in the Nordic countries: a questionnaire survey from 5739 members of the psoriasis associations data from the Nordic Quality of Life Study, *Acta Derm Venereol*, 2001, **81**, 116-121.
4. B. J. Nickoloff, The cytokine network in psoriasis, *Arch Dermatol*, 1991, **127**, 871-884.
5. T. Horio, Indications and action mechanisms of phototherapy, *J Dermatol Sci*, 2000, **23 Suppl 1**, S17-21.
6. T. Mudigonda, T. S. Dabade and S. R. Feldman, A review of targeted ultraviolet B phototherapy for psoriasis, *J Am Acad Dermatol*, 2012, **66**, 664-672.
7. A. Menter and C. E. Griffiths, Current and future management of psoriasis, *Lancet*, 2007,

- 370**, 272-284.
8. E. Racz, E. P. Prens, D. Kurek, M. Kant, D. de Ridder, S. Mourits, E. M. Baerveldt, Z. Ozgur, I. W. F. van, J. D. Laman, F. J. Staal and L. van der Fits, Effective treatment of psoriasis with narrow-band UVB phototherapy is linked to suppression of the IFN and Th17 pathways, *J Invest Dermatol*, 2011, **131**, 1547-1558.
  9. J. Gui, M. Gober, X. Yang, K. V. Katlinski, C. M. Marshall, M. Sharma, V. P. Werth, D. P. Baker, H. Rui, J. T. Seykora and S. Y. Fuchs, Therapeutic Elimination of the Type 1 Interferon Receptor for Treating Psoriatic Skin Inflammation, *J Invest Dermatol*, 2016, **136**, 1990-2002.
  10. H. L. Ma, S. Liang, J. Li, L. Napierata, T. Brown, S. Benoit, M. Senices, D. Gill, K. Dunussi-Joannopoulos, M. Collins, C. Nickerson-Nutter, L. A. Fouser and D. A. Young, IL-22 is required for Th17 cell-mediated pathology in a mouse model of psoriasis-like skin inflammation, *J Clin Invest*, 2008, **118**, 597-607.
  11. K. Wolk, E. Witte, E. Wallace, W. D. Docke, S. Kunz, K. Asadullah, H. D. Volk, W. Sterry and R. Sabat, IL-22 regulates the expression of genes responsible for antimicrobial defense, cellular differentiation, and mobility in keratinocytes: a potential role in psoriasis, *Eur J Immunol*, 2006, **36**, 1309-1323.
  12. R. Sestito, S. Madonna, C. Scarponi, F. Cianfarani, C. M. Failla, A. Cavani, G. Girolomoni and C. Albanesi, STAT3-dependent effects of IL-22 in human keratinocytes are counterregulated by sirtuin 1 through a direct inhibition of STAT3 acetylation, *FASEB J*, 2011, **25**, 916-927.
  13. R. M. Andres, A. Hald, C. Johansen, K. Kragballe and L. Iversen, Studies of Jak/STAT3 expression and signalling in psoriasis identifies STAT3-Ser727 phosphorylation as a modulator of transcriptional activity, *Exp Dermatol*, 2013, **22**, 323-328.
  14. T. R. Kwon, J. H. Kim, J. Y. Hong, J. Seok, J. M. Kim, D. H. Bak, M. J. Choi, S. K. Mun, C. W. Kim and B. J. Kim, Irradiation with 310 nm and 340 nm ultraviolet light-emitting-diodes can improve atopic dermatitis-like skin lesions in NC/Nga mice, *Photochem Photobiol Sci*, 2018, **17**, 1127-1135.
  15. K. El Malki, S. H. Karbach, J. Huppert, M. Zayoud, S. Reissig, R. Schuler, A. Nikolaev, K. Karram, T. Munzel, C. R. Kuhlmann, H. J. Luhmann, E. von Stebut, S. Wortge, F. C. Kurschus and A. Waisman, An alternative pathway of imiquimod-induced psoriasis-like skin inflammation in the absence of interleukin-17 receptor a signaling, *J Invest Dermatol*, 2013, **133**, 441-451.
  16. W. Zhang, E. Dang, X. Shi, L. Jin, Z. Feng, L. Hu, Y. Wu and G. Wang, The pro-inflammatory cytokine IL-22 up-regulates keratin 17 expression in keratinocytes via STAT3 and ERK1/2, *PLoS One*, 2012, **7**, e40797.
  17. J. A. Parrish and K. F. Jaenicke, Action spectrum for phototherapy of psoriasis, *J Invest*



- Dermatol*, 1981, **76**, 359-362.
18. H. Valdimarsson, B. S. Bake, I. Jonsdottr and L. Fry, Psoriasis: a disease of abnormal Keratinocyte proliferation induced by T lymphocytes, *Immunol Today*, 1986, **7**, 256-259.
  19. F. Aubin, Mechanisms involved in ultraviolet light-induced immunosuppression, *Eur J Dermatol*, 2003, **13**, 515-523.
  20. W. Lapolla, B. A. Yentzer, J. Bagel, C. R. Halvorson and S. R. Feldman, A review of phototherapy protocols for psoriasis treatment, *J Am Acad Dermatol*, 2011, **64**, 936-949.
  21. C. Green, J. Ferguson, T. Lakshmipathi and B. E. Johnson, 311 nm UVB phototherapy--an effective treatment for psoriasis, *Br J Dermatol*, 1988, **119**, 691-696.
  22. B. Bonis, L. Kemeny, A. Dobozy, Z. Bor, G. Szabo and F. Ignacz, 308 nm UVB excimer laser for psoriasis, *Lancet*, 1997, **350**, 1522.
  23. Y. Zhuang, C. Han, B. Li, L. Jin, E. Dang, H. Fang, H. Qiao and G. Wang, NB-UVB irradiation downregulates keratin-17 expression in keratinocytes by inhibiting the ERK1/2 and STAT3 signaling pathways, *Arch Dermatol Res*, 2018, **310**, 147-156.
  24. H. Yu, D. Pardoll and R. Jove, STATs in cancer inflammation and immunity: a leading role for STAT3, *Nat Rev Cancer*, 2009, **9**, 798-809.
  25. B. B. Ding, J. J. Yu, R. Y. Yu, L. M. Mendez, R. Shaknovich, Y. Zhang, G. Cattoretti and B. H. Ye, Constitutively activated STAT3 promotes cell proliferation and survival in the activated B-cell subtype of diffuse large B-cell lymphomas, *Blood*, 2008, **111**, 1515-1523.
  26. G. Niu, K. L. Wright, M. Huang, L. Song, E. Haura, J. Turkson, S. Zhang, T. Wang, D. Sinibaldi, D. Coppola, R. Heller, L. M. Ellis, J. Karras, J. Bromberg, D. Pardoll, R. Jove and H. Yu, Constitutive Stat3 activity up-regulates VEGF expression and tumor angiogenesis, *Oncogene*, 2002, **21**, 2000-2008.
  27. L. Bao, H. Zhang and L. S. Chan, The involvement of the JAK-STAT signaling pathway in chronic inflammatory skin disease atopic dermatitis, *JAKSTAT*, 2013, **2**, e24137.
  28. L. Kemeny, Z. Csoma, E. Bagdi, A. H. Banham, L. Krenacs and A. Koreck, Targeted phototherapy of plaque-type psoriasis using ultraviolet B-light-emitting diodes, *Br J Dermatol*, 2010, **163**, 167-173.
  29. J. M. Tarrant, Blood cytokines as biomarkers of in vivo toxicity in preclinical safety assessment: considerations for their use, *Toxicol Sci*, 2010, **117**, 4-16.





(e) Relative protein ratios were determined as band intensities with pS-STAT3 and p-ERK ratios in each irradiation group relative to the control. Significant differences from the control group are indicated by \* $P < 0.05$ , \*\* $P < 0.01$ , and \*\*\* $P < 0.001$  versus unirradiated cells. (f) Representative images of immunocytochemical staining by anti-pS-STAT3 (green) for pS-STAT3 in HaCaT cells irradiated with indicated energy levels of 310 nm (50 mJ/cm<sup>2</sup>) for 24 h. Cells were counterstained with DAPI (blue) before mounting. Significant differences from the control group are indicated as \* $P < 0.05$ , \*\* $P < 0.01$ , and \*\*\* $P < 0.001$  versus unirradiated cells.

266x119mm (300 x 300 DPI)

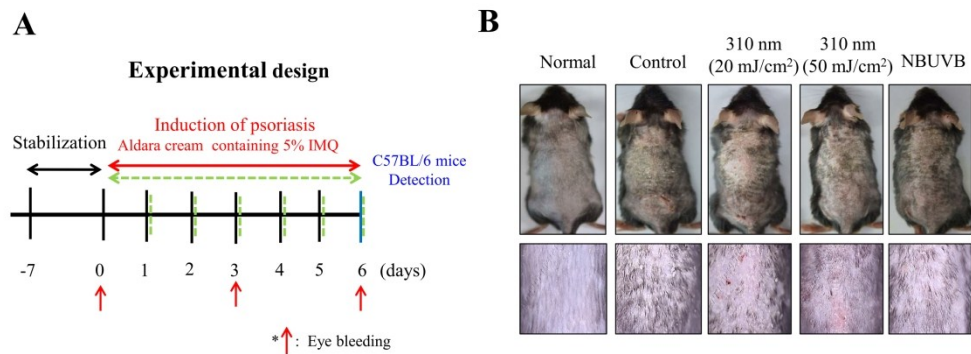
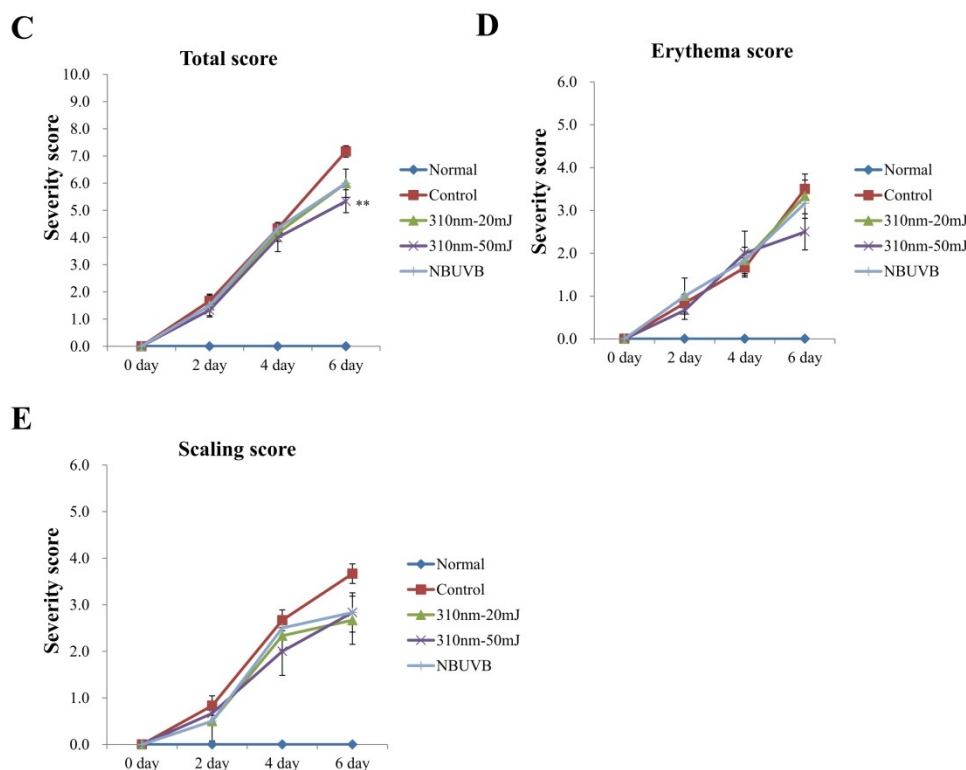


Fig. 2 Experimental induction of imiquimod-induced psoriasis-like skin inflammation and clinical changes in imiquimod (IMQ)-treated mouse skin The back skin and right ear of mice were treated with commercially available IMQ cream (5%; Aldara, 3M Pharmaceuticals, UK) for 6 consecutive days at a daily dose of 80 mg, which contained 4 mg of the active compound. After application, mice were exposed to UV-LED (310 nm) and NB-UVB every other day. (b) Mice were divided into five groups: G1, Normal; G2, Control (IMQ-applied only); G3, 310 nm 20 mJ/cm<sup>2</sup>; G4, 310 nm 50 mJ/cm<sup>2</sup>; and G5, NB-UVB. Normal mice (left) showed no changes in skin lesions. IMQ-treated mice showed psoriasis-like skin lesions with erythema, thickness, and scale. The picture is representative of the six IMQ group mice.

266x102mm (300 x 300 DPI)



(c, d, e) Psoriasis-like skin lesions were clinically evaluated by PASI scores: erythema increased from day 1 to 6, scaling was observed on day 3 and gradually increased until day 6, and the thickness was observed to increase from day 2 to 6. Data are presented as means $\pm$ SD of changes in values. \*\* $p < 0.01$  compared to the controls ( $n=6$ ).

266x212mm (300 x 300 DPI)

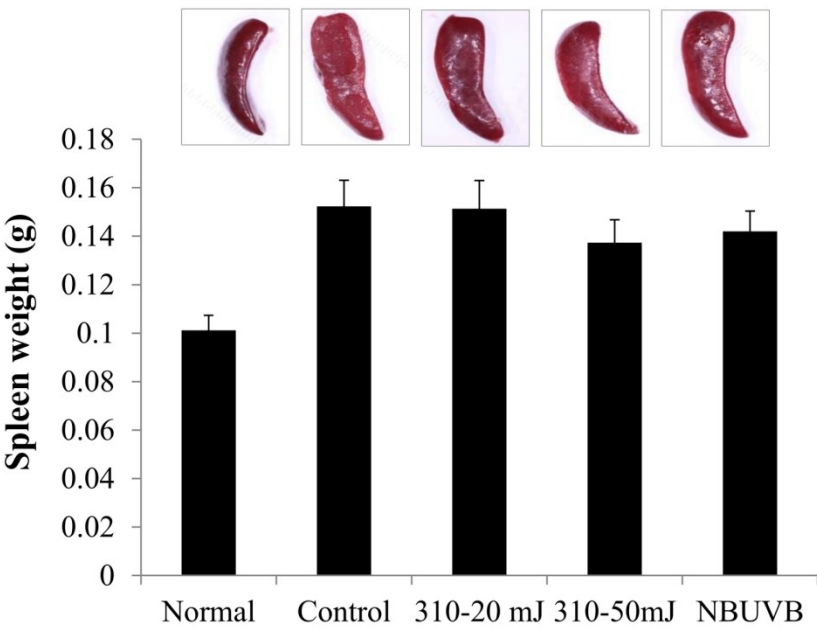


Fig. 3 Effect of UV-LED irradiation on spleen size and weight (a) Mice were sacrificed on day 6 for serum collection after 6 days. Spleen sizes were weighed at sacrifice and compared by direct viewing of representative images. Bar graphs represent the mean $\pm$ SD, with six mice per group. Data shown are representative of three experiments.

160x127mm (300 x 300 DPI)

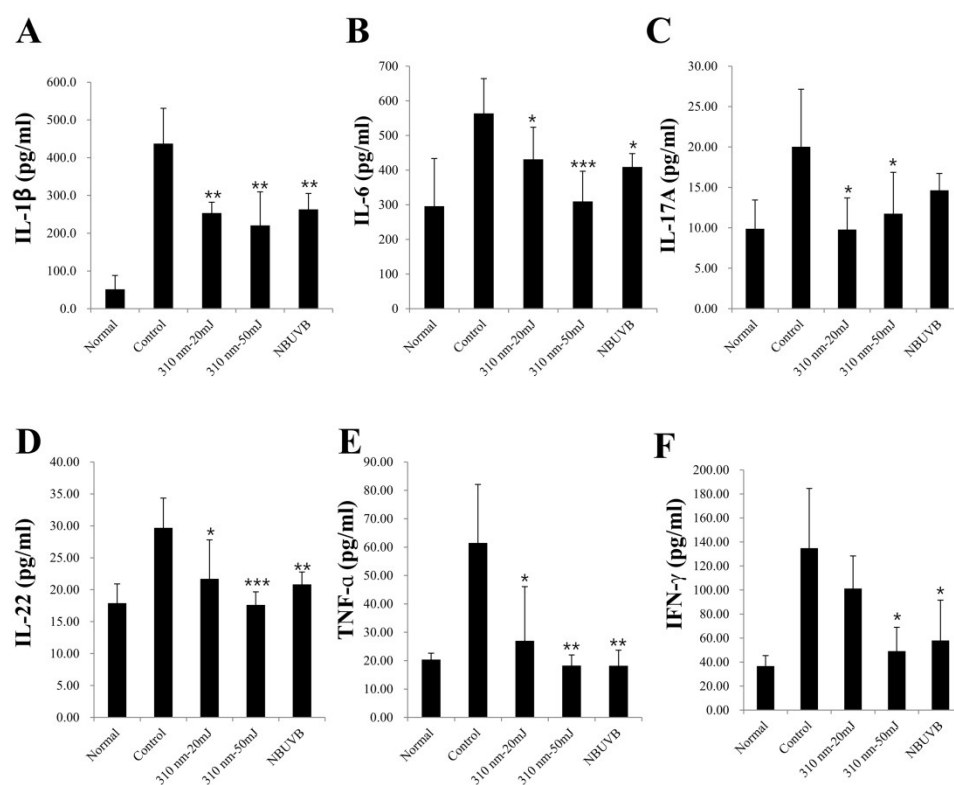


Fig 4. Effects of UV-LED irradiation on serum cytokine levels in imiquimod (IMQ)-treated mice. The serum levels of (a) IL-1 $\beta$ , (b) IL-6, (c) IL-17A, (d) IL-22, (e) TNF- $\alpha$ , and (f) IFN- $\gamma$  were measured. Inflammatory cytokine levels were measured using ELISA kits. Data are presented as means $\pm$ SD of changes in values. \* $p$ <0.05 and \*\* $p$ <0.01 compared to the controls ( $n$ =6).

266x220mm (300 x 300 DPI)

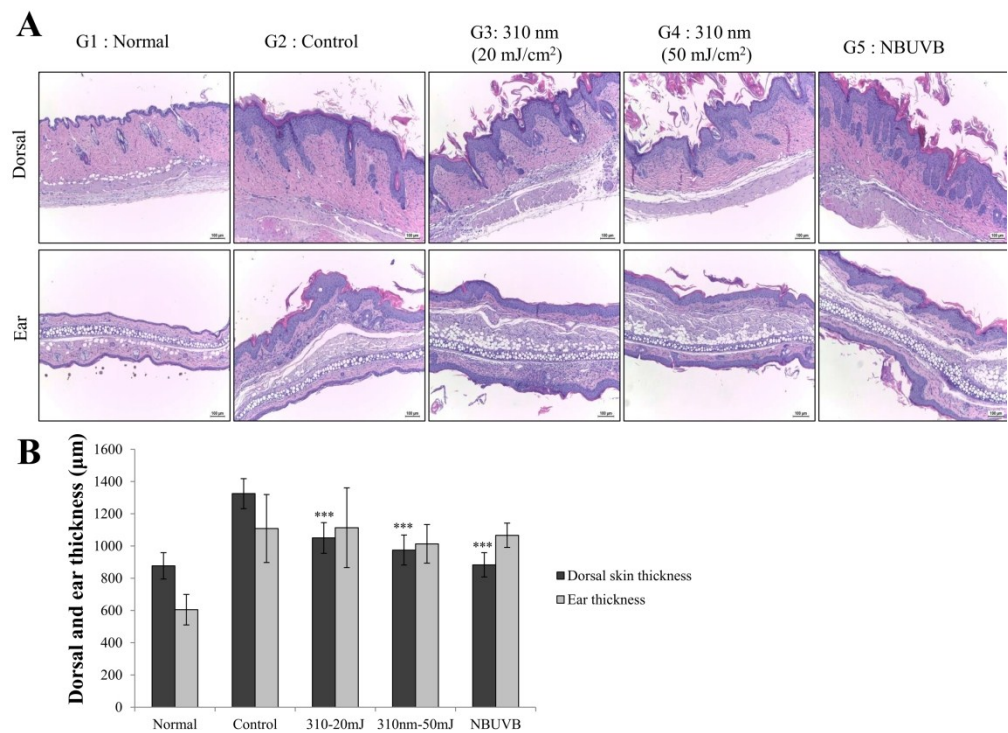
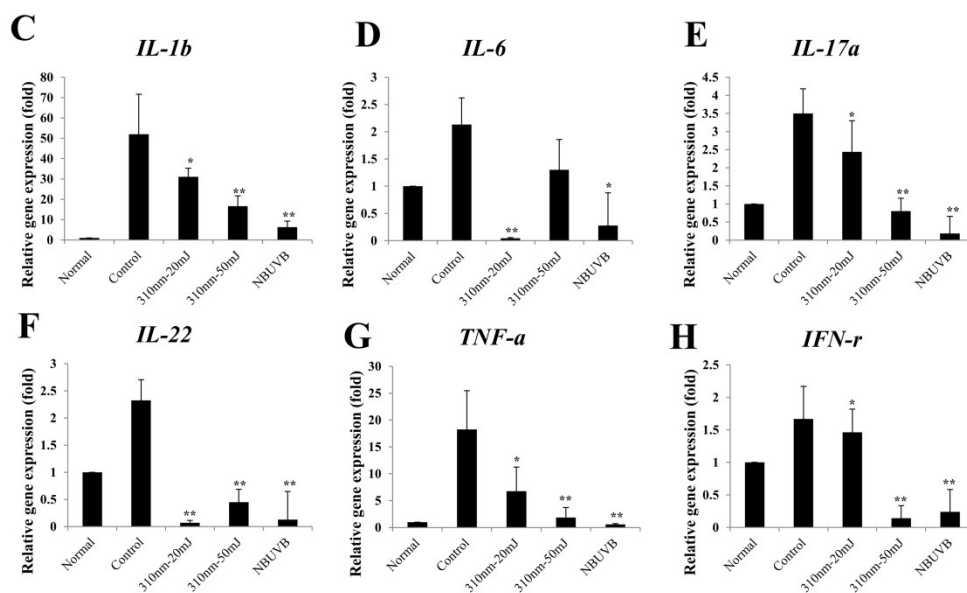


Fig. 5 Improvement of the imiquimod-induced psoriasiform dermatitis in mice by 310-nm UV-LED is associated with suppression of Th cell-associated inflammatory cytokines (a) H&E staining of the IMQ-treated back skin section shows psoriasis-like changes including scaling, epidermal thickness, keratinocyte hyperproliferation, and granulocyte infiltration compared to control back and ear skin. A representative picture of six mice is shown. H&E-stained paraffin sections were observed at original magnification ( $\times 100$ ). (b) Dorsal and ear skin thickening measurements were performed using an optical microscope. Normal control animals received neither IMQ nor vehicle cream.

266x195mm (300 x 300 DPI)





The mRNA levels of (c) IL-1 $\beta$ , (d) IL-6, (e) IL-17A, (f) IL-22, (g) TNF- $\alpha$ , and (h) IFN- $\gamma$  were revealed by real-time quantitative RT-PCR (qRT-PCR). Data are presented as means $\pm$ SD of changes in values. \* $p$ <0.05 and \*\* $p$ <0.01 compared to the controls ( $n$ =6).

266x160mm (300 x 300 DPI)

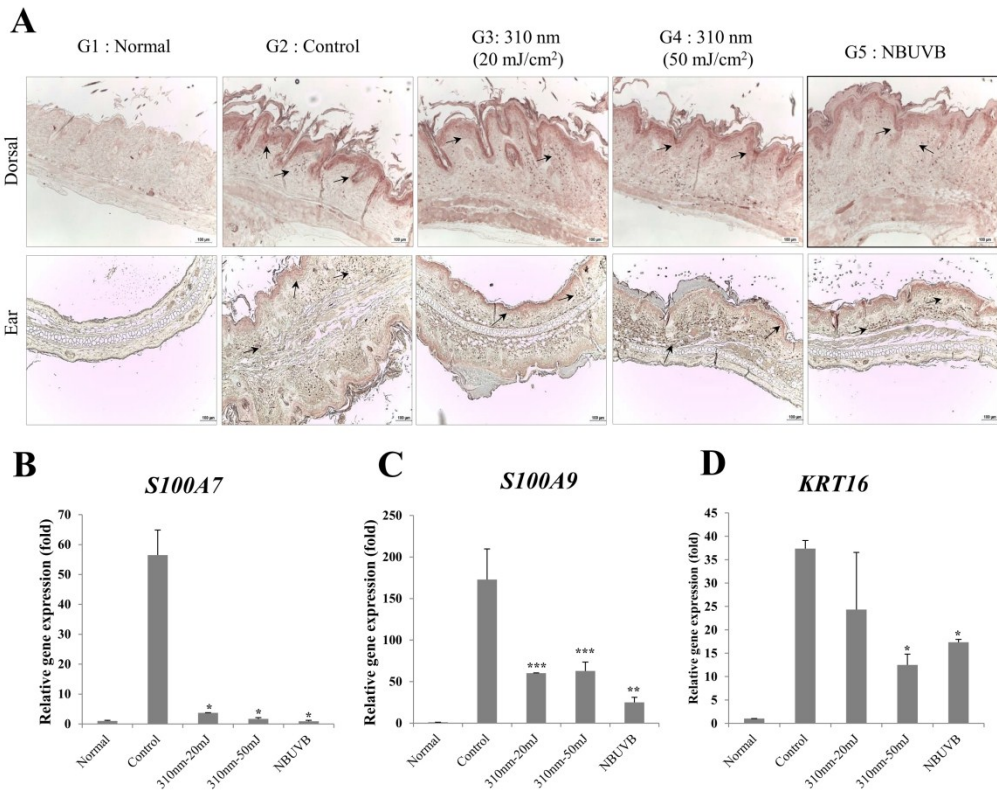


Fig. 6 Improvement of psoriasis-like skin disease via S100A9 suppression in imiquimod-induced mice after treatment with 310 nm UV-LED. (a) Immunohistochemical analysis was performed for S100A9 protein in the back and ear skin of psoriatic mice, and UV-LED irradiation could effectively decrease S100A9 protein expression (×100). The mRNA levels of (b) S100A7, (c) S100A9, and (d) Keratin 16 were revealed by real-time quantitative RT-PCR (qRT-PCR). The data are presented as means±SD of changes in values. \*p<0.05 and \*\*p<0.01 compared to the controls (n=6).

266x228mm (300 x 300 DPI)

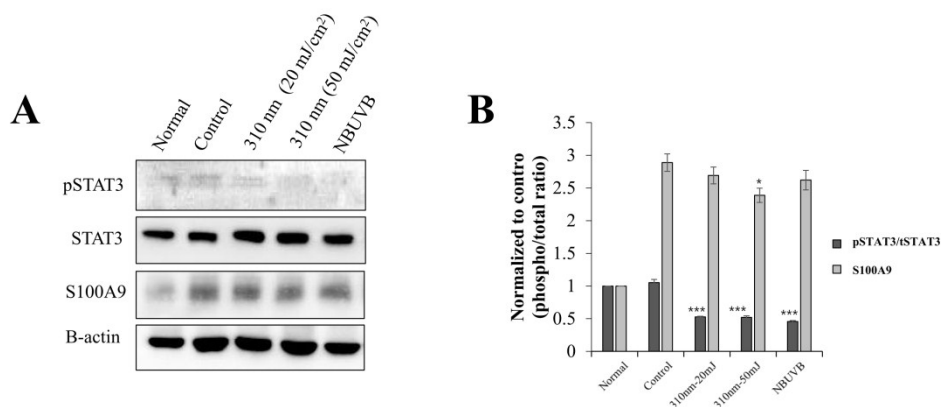
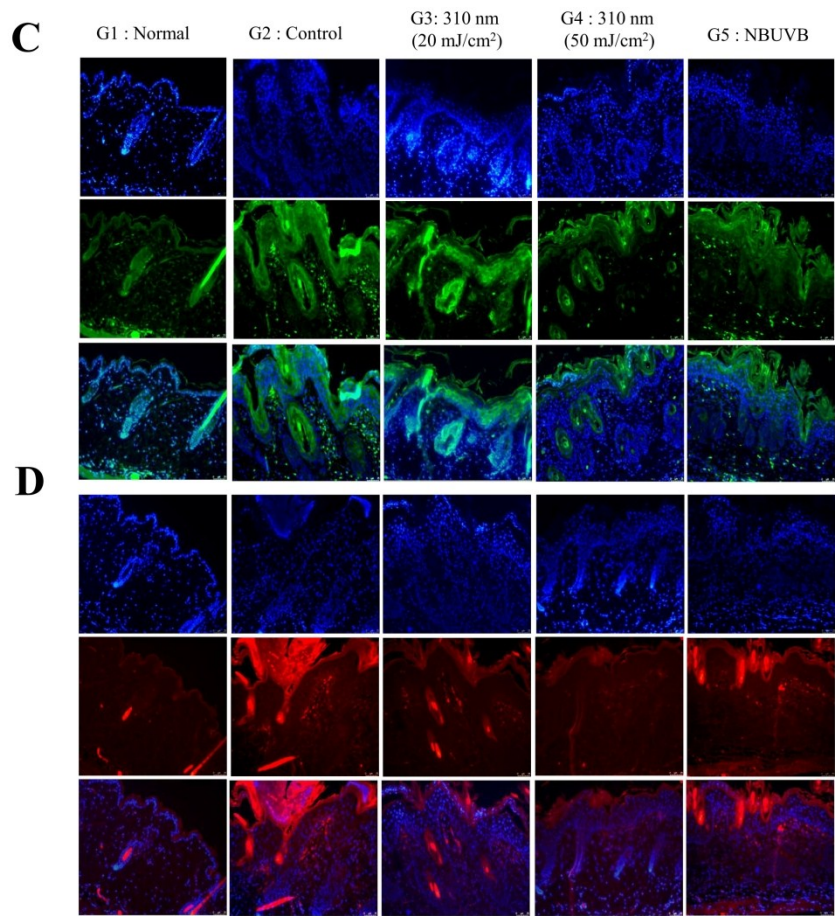


Fig. 7 Irradiation of 310 nm UV-LED suppressed skin inflammation via STAT3/S100A9 in imiquimod-induced mice. (a) Tissue extracts from mouse back skins were prepared and blotted to evaluate pS-STAT3, total STAT3, and S100A9 expression. (b) Relative protein ratios were determined as band intensities with ratios of pS-STAT3 and S100A9 in each irradiation group relative to the control. Significant differences from the control group are \* $P < 0.05$ , \*\*\* $P < 0.001$  versus the control group.

266x110mm (300 x 300 DPI)



(c) S100A9 and (d) pS-STAT3 protein localization was visualized in each group under a fluorescence microscope after staining with each antibody and FITC-labelled secondary antibody (green). The cell nuclei were stained with DAPI (×100). Images are representative of three independent experiments.

266x244mm (300 x 300 DPI)

**Table1. Primer sequence information used in qRT-PCR**

Gene	Sequences	
IL-1 $\beta$	Forward	5'- CAACCAACAAGTGATATTCTCCATG -3'
	Reverse	5'- GATCCACACTCTCCAGCTGCA -3'
IL-6	Forward	5'- GAGGATACCACTCCCAACAGACC -3'
	Reverse	5'- AAGTGCATCATCGTTGTTCATACA -3'
IL-17A	Forward	5'- TTTTCAGCAAGGAATGTGGA -3'
	Reverse	5'- TTCATTGTGGAGGGCAGAC -3'
IL-22	Forward	5'- TGACGACCAGAACATCCAGA -3'
	Reverse	5'- CGCCTTGATCTCTCCACTCT -3'
TNF- $\alpha$	Forward	5'- CATCTTCTCAAAATTCGAGTGACAA -3'
	Reverse	5'- TGGGAGTAGACAAGGTACAACCC -3'
IFN- $\gamma$	Forward	5'- GGCCATCAGCAACAACATAAG -3'
	Reverse	5'- GTTGACCTCAAACCTTGGCAATAC -3'
GAPDH	Forward	5'- AGCTTGTCATCAACGGGAAG -3'
	Reverse	5'- TTTGATGTTAGTGGGGTCTCG -3'